

Implementation of MEMS Accelerometer for Velocity-based Seismic Sensor

Amalia C. Nur'aidha
Physics Master Program
Brawijaya University

Jl. Veteran Malang 65145, Indonesia
 amaliacemara@student.ub.ac.id

Sukir Maryanto
Dept. of Physics

Brawijaya University
 Jl. Veteran Malang 65145, Indonesia
 sukir@ub.ac.id

Didik R. Santoso*
Dept of Physics

Brawijaya University
 Jl. Veteran Malang 65145, Indonesia
 dieks@ub.ac.id

*Corresponding Author

Abstract— Micro Electro Mechanical System (MEMS) accelerometer is commonly used as acceleration-based vibration sensor. The MEMS accelerometer is small device, simple in the implementation design, and relatively inexpensive. But in some fields of application, due to low frequency operation and also small magnitude of the measured signal, for example in seismology, velocity-based vibration sensor is usually more desirable than acceleration-based sensor. In this research, a velocity-based vibration sensor has been developed using MEMS Accelerometer device e.g. MMA7361L. The acceleration-based vibration signal from the MMA7361L is converted into a velocity-based vibration signal by using an integrator circuit module. This module is assembled by using a band-pass filter and an integral-amplifier. The laboratory test shows that the developed sensor system could detect both low and high-frequency vibration signals in velocity-based with good result. The sensor system has a frequency range of 0.02Hz to 148Hz. It is wider frequency than the geophone (seismic sensor), thus the velocity-based MEMS sensor system has capability for geophone replacement.

Keywords—MEMS accelerometer, velocity-based sensor, integrator

I. INTRODUCTION

A vibration sensor for detection seismic wave is called a seismic sensor. It is a main component in seismology, which normally used for monitoring seismic activities and seismic explorations [1]. The sensor able to transfer the ground motion into electrical signals [2]. A seismic sensor serves as velocity or acceleration of ground vibrations which is on the surface of the earth [3]. Several seismic sensors have been developed based sensing of an accelerometer, piezoelectric, electromagnetic, capacitance, and others [1].

Usually, the seismic sensors were often used for seismic exploration is geophone. It is one type of electromagnetic spring sensors, which the working principle of it is velocity-

based vibration. Geophone sensor has good linearity and has a relatively low ground noise. However, it has a problem that the limited linear frequency range above natural frequency, usually at 4-12Hz [4].

Recently, great interest of an alternative technology in seismic sensor is MEMS accelerometer device. It is a microchip shaped and acceleration-based sensing device [5]. MEMS accelerometer sensor has ability to detect vibrations-acceleration in broad frequencies, e.g. at 0-800Hz [7]. Unlike geophone which is works above the resonance frequency of velocity, MEMS accelerometers work under the resonant frequency of acceleration. Because of MEMS accelerometer is acceleration-based sensor, it is suitable for strong motion vibration (seismic) sensor, e.g. for high magnitude and high frequency signals [9]. For weak and low-frequency signals, when ground motion occurs at almost the constant velocity the MEMS accelerometer sensor maybe no detects the signals. It is disadvantage of using MEMS accelerometer as acceleration-based sensor for seismic signals. Therefore, in this research we propose a simple method and circuit to convert acceleration-based sensor to velocity-based sensor of the MEMS accelerometer device. So that the weak and low frequency vibration seismic signal can be detected by using MEMS accelerometer based sensor.

II. METHODS

Fig. 1 shows the block diagram of the integrated sensor system developed in this research. In this research, used MEMS Accelerometer MMA7361L sensor in the form of IC chip. MMA7361L are analog sensors fabricated by Freescale Semiconductor. The MMA7361L sensor enables signal conditioning and g-select to select two sensitivities (1.5g and 6g), with a maximum sensitivity of 800mV / g@1.5g. In addition, the MMA7361L sensor has three working components vertically and horizontally (x, y, and z) [10]. In this study only used the z component that moves vertically. The output then connected to the conditioning circuit.

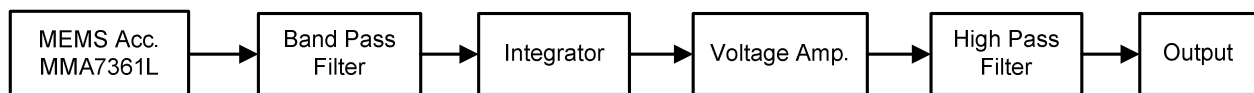


Fig. 1. Block diagram of velocity-based vibration sensor system

Before developing the signal conditioning circuit of the MMA7361L sensor first the geophone sensor simulated to determine the frequency response into the reference (Fig. 2a). Based on Fig. 2a it appears that geophones work at high frequencies with a frequency range at 10Hz until 100Hz and it cannot respond to vibrations when below 10Hz. Geophone inability to respond to frequencies below 10 Hz because the signal recorded is passed on a high pass to reduce the noise around the sensor. Moreover, it cannot be done bandwidth expansion to very low frequencies. Furthermore, Fig. 2a

shows that if the low frequency recorded by geophone its amplitude will decrease [5]. It indicated the geophone deficiency which makes opportunity for MEMS Accelerometer sensor already has a wider frequency bandwidth. The MMA7361L frequency response in Fig. 2b range at 0.01Hz to 200Hz. These show that a flat response amplitude in acceleration. Furthermore, an integral process needed to convert the signal from acceleration into velocity. Then it will be amplified and filtering to obtain the desired frequency range.

This research is funded by the Directorate of Research and Community Service, Ministry of Research, Technology, and Higher Education based on contract no: 054/SP2H/LT/DRPM/2018.

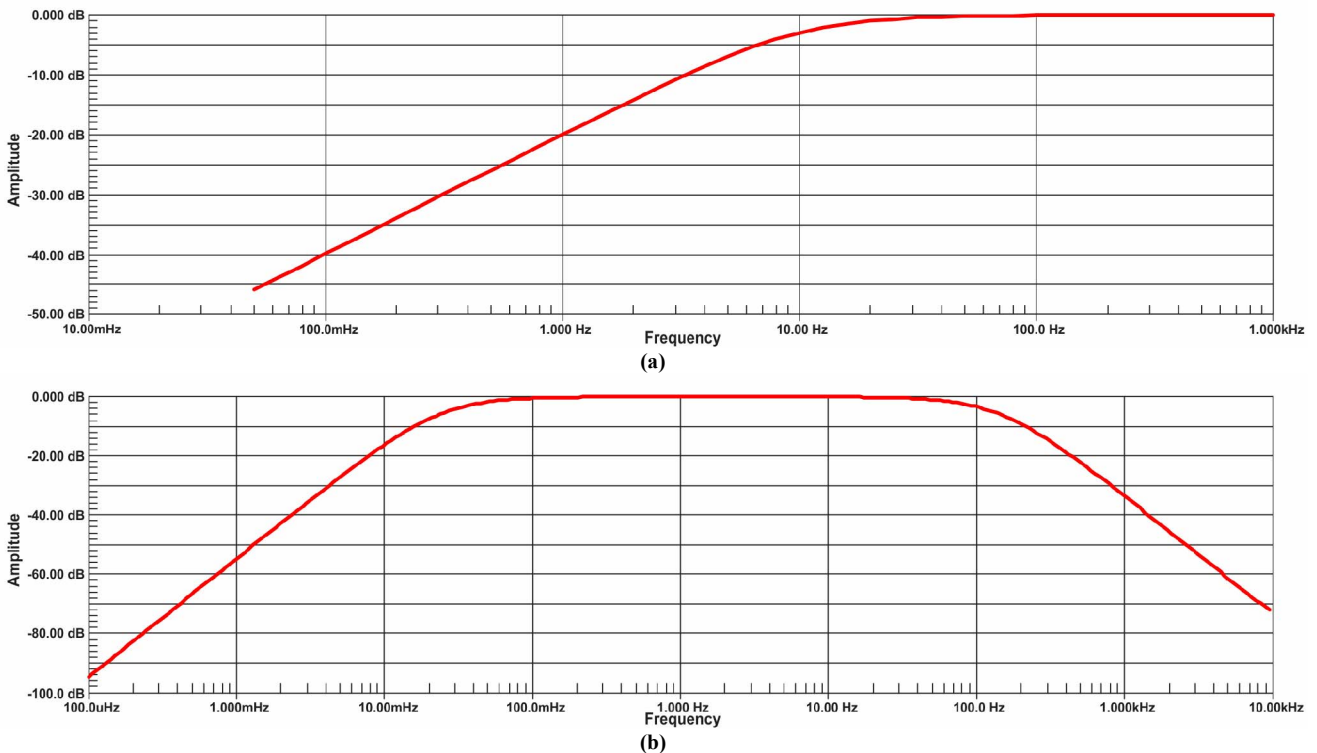


Fig. 2. Frequency response of (a) Geophone and (b) MEMS accelerometer

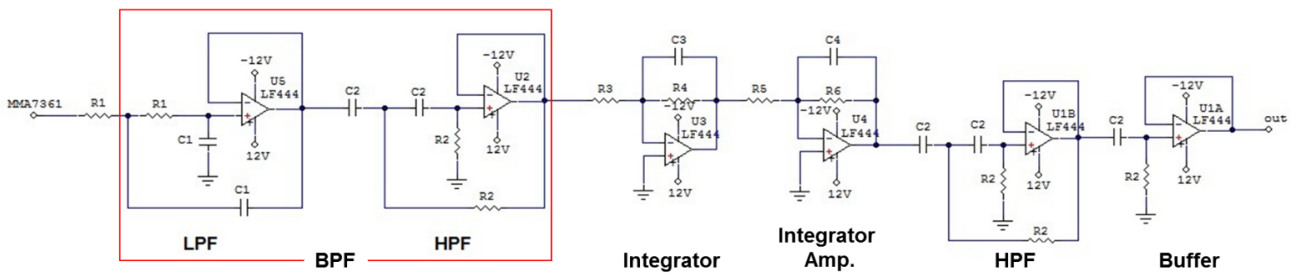


Fig. 3. The signal conditioning circuit for the vibration sensor

Implementation of the block diagram of Fig 1 showed by a circuit in Fig. 3. The circuit in Fig. 3 is composed of the Band Pass Filter (BPF) series which consist by Low Pass Filter (LPF) and High Pass Filter (HPF) circuits then it assembled by the integrator, amplifier, High Pass Filter, and buffer series. The LPF and HPF circuits which form the BPF series is designed based on Sallen-Key second order filter and using the LF444 IC. LF444 is a low power op-amp IC and has a bandwidth up to 1MHz, besides LF444 it is also built from 4 op-amps in one IC [11]. Each f_{c-LPF} and f_{c-HPF} values are determined by Equation (1) and (2). Both of these frequencies become more specific by setting the value of (R_1 , C_1) and (R_2 , C_2).

$$f_{c-LPF} = \frac{1}{2\pi\sqrt{R_1 R_1 C_1 C_1}} = \frac{1}{2\pi R_1 C_1} \quad (1)$$

$$f_{c-HPF} = \frac{1}{2\pi\sqrt{R_2 R_2 C_2 C_2}} = \frac{1}{2\pi R_2 C_2} \quad (2)$$

Then BPF series connected to the integrator circuit. The function of integrator circuit is to change the acceleration signal into velocity signal. Basic the integrator circuit (Fig. 4) has assembled by placing the capacitor (C) in the feedback

loop. If the circuit assumed as an ideal op-amp, then the Equation 3 is used [12].

$$I_R = I_C$$

$$\frac{V_{in}}{R} = -C \frac{dV_{out}}{dt} \quad (3)$$

Integral from 0 to t then Equation (3) become Equation (4)

$$\int dV_{out} = -\int \frac{V_{in} \tau}{RC} d\tau \quad (4)$$

$$V_{out} = -\frac{1}{RC} \int V_{in}(\tau) d\tau + V_{out}(0)$$

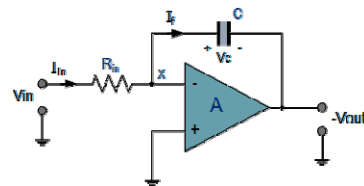


Fig. 4. Ideal integrator circuit

Frequency domain analysis obtained by expressing impedance feedback component in the complex plane, then the transfer function can thus be written as Equation 5. Equation 5 shows that different phase 90° between the input and output occurs at all frequencies.

$$\frac{V_{out}}{V_{in}} = -\frac{Z_c}{Z_R} = \frac{j\omega C}{R} = \frac{j}{\omega RC} \quad (5)$$

For DC signals at $\omega = 0$ and unlimited gain in the integrator circuit become equivalent like an open circuit. The slackening of feedback from the capacitor made drift in

output voltage due to the input DC voltage had offset. The problem can be solved by connecting a resistor R_f in parallel with the feedback capacitor (C) (Fig. 5) so obtained the equation (6) [13].

$$V_{in} = A \sin(\omega t) \quad (6)$$

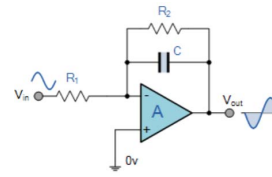


Fig. 5. Integrator circuit

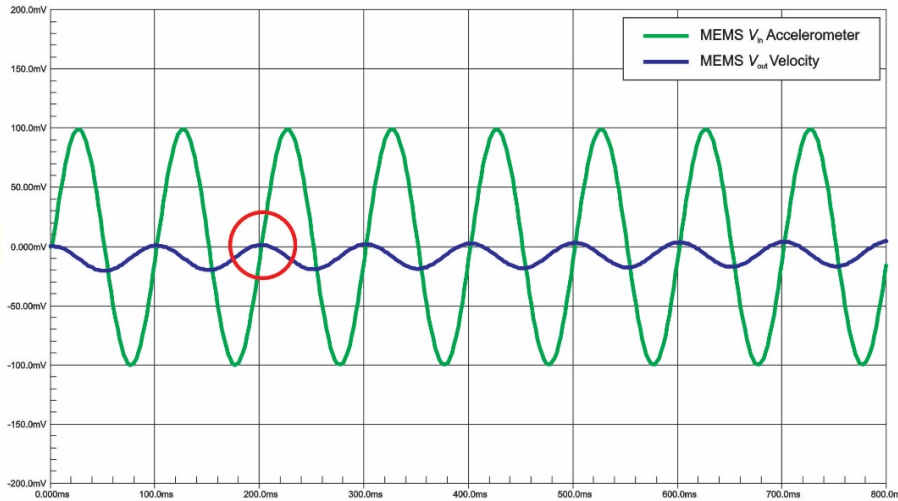


Fig. 6. Response signal input (green line) and output (yellow line) of MEMS-integrator circuit.

The simulation result using integrator circuit as shown in Fig. 6. An input signal has an acceleration (green line) then given integrator circuit so that the output signal becomes the velocity signal (yellow line). The circle sign in Fig. 6 shows the signal change from the acceleration into the velocity signal. The integrator circuit built on this research uses LF444 IC just like in previous LPF and HPF circuit.

$$V_{out} = \int V_{in} dt = \int A \sin(\omega t) = -A \cos(\omega t) \quad (7)$$

Then the velocity signal result from integrator circuit will be connected to the integrator amplifier circuit. The function of the integrator amplifier to amplify the output voltage of the integrator circuit. In this research, the Integrator amplifier circuit is built using LF444 IC. Determination of the gain is given by equation 8 and setting (R_5 , R_6) value to obtain the more specific gain value.

$$A_v = \frac{R_6}{R_5} \quad (8)$$

Then, the amplifier output voltage connected to the HPF circuit for passing the high frequency and reduce the incoming mechanical noises. Last, there is a buffer circuit that used to keep the voltage always stable. The output of the signal conditioning circuit will be connecting to the S5000 Pico-scope (4 channels) which an entire Pico-scope process controlled by its software already installed on the computer.

III. RESULT AND DISCUSSION

Implementation of the sensor and signal conditioning circuit that has been developing printed on PCB (Fig. 7). The

MMA7361L sensor attached to the cantilever beam that used for the sensor test tool. Based on Fig. 7a, there are three output channels (x, y, and z components) from the sensor but in this research only used one channel (z or vertical component). The z component has three pins that consisting of one pin for z output and two other pins as a power supply (ground and 5V). The output from the sensor connected to the signal conditioning module (Fig. 7b). The module consists of three circuits include the low-frequency velocity circuit, high-frequency velocity circuit, and acceleration signal conditioning circuit. Those three circuits are consist of BPF, integrator, integrator amplifier, HPF, and buffer. Except, for the acceleration signal conditioning circuit is not equipped by the integrator circuit because it's just used as a comparison.

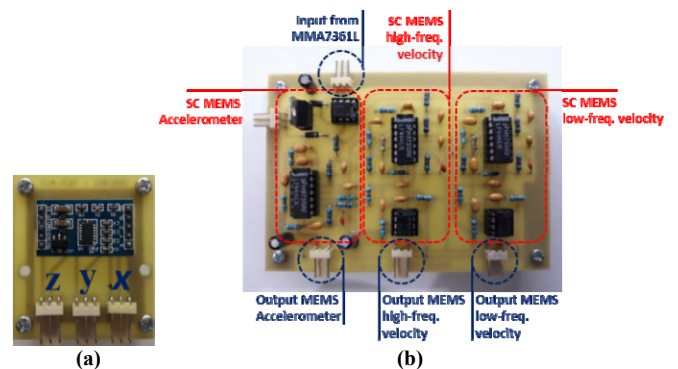


Fig. 7. Design result on PCB (a) MEMS accelerometer MMA7361L sensor and (b) integrated signal conditioning circuit

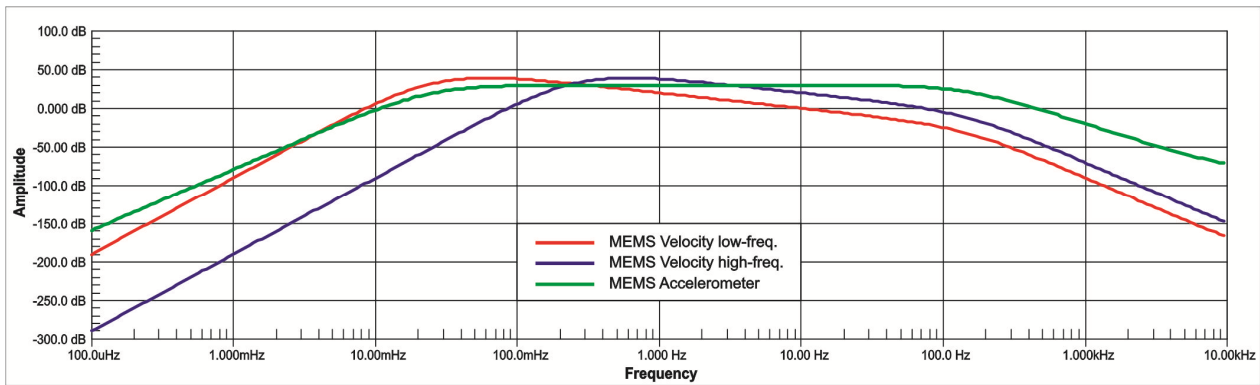


Fig. 8. Frequency responses from MEMS velocity low-frequency (green), high-frequency (red), and MEMS accelerometer (blue)

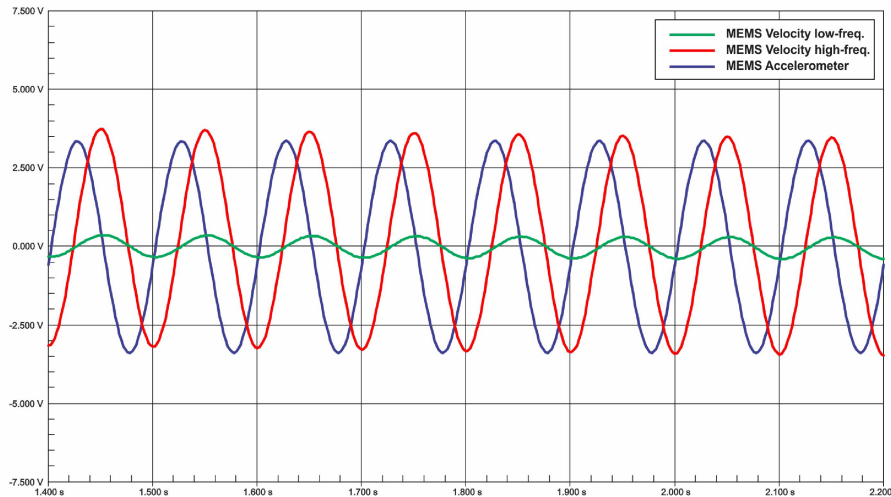


Fig. 9. Signal responses from MEMS velocity low-frequency (green), high-frequency (red) and MEMS accelerometer (blue)

Several simulations are performed to determine the performance of the sensor system has been built based on the circuit in Fig. 3. This performance determination is done by setting the values of $R_1 = 3.3k\Omega$; $C_1 = 330nF$; $R_2 = 680k\Omega$ and $C_2 = 10\mu F$, the LPF cut-off frequency value is 146Hz and HPF cut-off is 0.02Hz. With these results, the sensor system has a frequency range from 0.02Hz to 146Hz. This frequency range has used for low-frequency velocity circuit in signal conditioning module. Meanwhile, for the high frequency velocity circuit used $R_1 = 3.3k\Omega$; $C_1 = 330nF$; $R_2 = 680k\Omega$ and $C_2 = 10\mu F$ and it has a frequency range from 0.2Hz to 146Hz (Fig. 8). This range frequency usually designed for seismic sensors in general. Moreover, Fig. 9 shows the result of the simulation high and low-frequency output signals from signal conditioning velocity module then compared them with the high-frequency output from MEMS accelerometer circuit. While the signal voltage gain in this research refers to the equation 8 and setting the value of $R_5 = 10k$ and $R_6 = 330k\Omega$ thus gaining has obtained by 33 times (30dB).

The velocity signal response test from the sensor system observed by attaching the MMA7361L sensor on the cantilever beam by moving the cantilever edge so that obtained high and low-frequency vibrations. Fig. 10a shows the high-frequency output signal from the high-frequency velocity circuit gets maximum amplitude when the sensor system given by a high-frequency vibration type. Similarly, output amplitude response of the low-frequency velocity circuit indicates the presence of low-frequency signal response with maximum amplitude at the peak signal. It happens when high-frequency vibration propagates always

be followed by low-frequency vibration so that the sensor system successfully respond to the low-frequency vibration that oscillation with high-frequency. Meanwhile, for the signal response of high-frequency acceleration circuit has a fluctuated amplitude which reaches the maximum amplitude for a moment then gradually decreases. Then it is also done for low-frequency vibration in the signal response test. Fig. 10b shows the output signal response of low-frequency velocity circuit. The output signal amplitude is equal to acceleration circuit response and still response to the high-frequency vibrations oscillation with the low-frequency vibrations given during the test.

The signal response test result of the velocity-based MEMS sensor system with various vibration frequencies show that the sensor system was able to respond well to all signal frequencies. Next, the sensor system has tested by comparing signal response with the geophone. Fig. 11a is the testing result for high-frequency vibration, seen at the high frequency both velocity-based MEMS sensor system and geophone having the same amplitude value. It shows that at a high-frequency the velocity-based MEMS sensor system can detect vibration well and its ability is proportional to the geophone. Meanwhile, for the result of a low-frequency vibration response has shown in Fig. 11b where at this frequency velocity-based MEMS sensor system has greater amplitude value than geophone. It is due to the geophone is unable to detect low frequencies below 10Hz whereas the velocity-based MEMS sensor system has detectability ranging from 0.02 Hz.

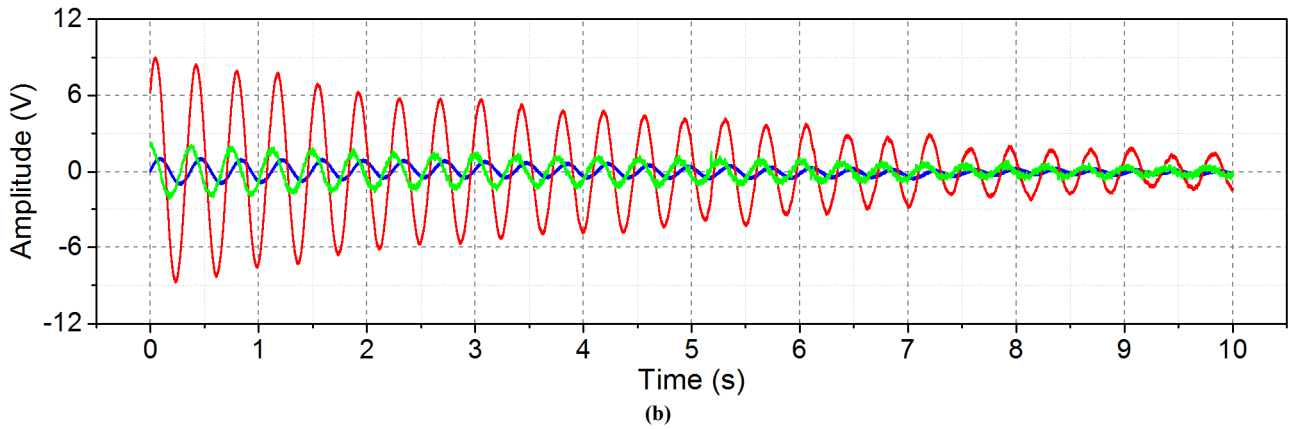
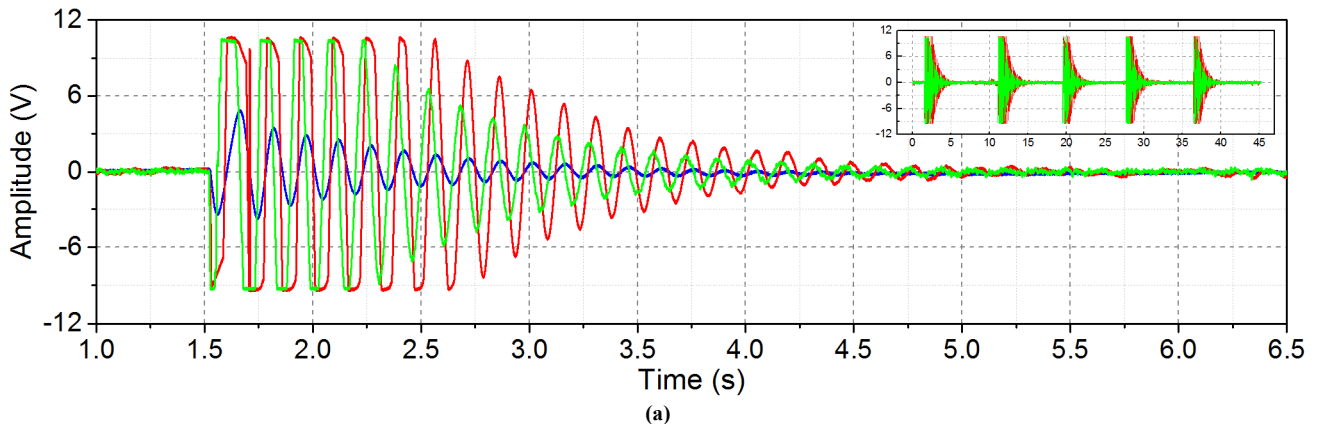


Fig. 10. Signal response of (a) high frequency and (b) low frequency vibrations from signal conditioning high-frequency velocity (red), low-frequency velocity (blue) and MEMS accelerometer (green) circuits.

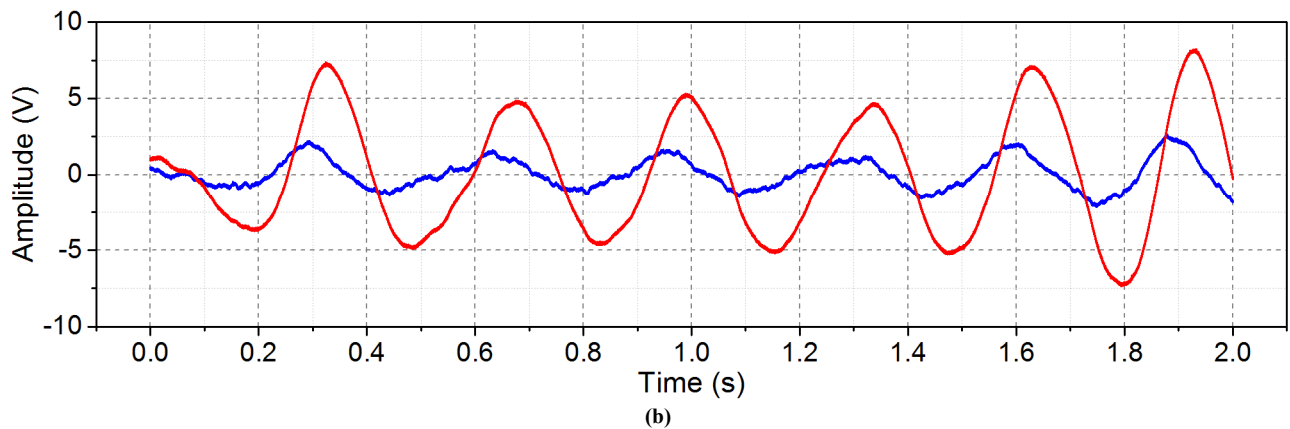
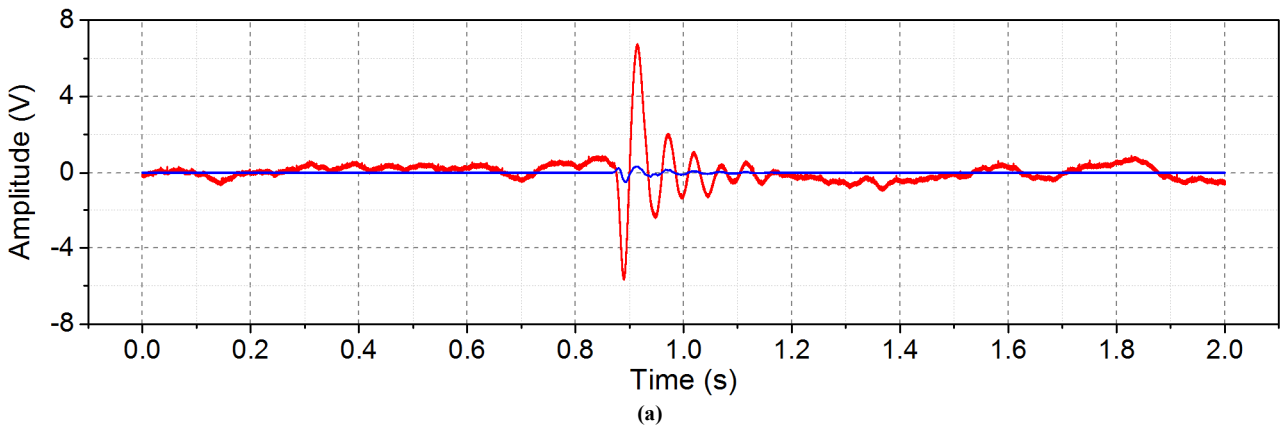


Fig. 11. Comparison (a) high-frequency and (b) low-frequency of velocity signal from velocity-based MEMS (red) and geophone (blue) sensor system.

IV. CONCLUSION

This research has successfully developed MEMS Accelerometer MMA7361L sensor as a velocity-based vibration sensor by designing a signal processing module capable of converting acceleration signal into velocity signals. The velocity signal output from the sensor system is more stable than geophone output. This based on the amplitude response test results for both sensors while given by the low and high-frequency vibration. As geophones as this system have also been able to detect low-frequency signals that oscillate along with high-frequency vibration signals and vice versa. Other capabilities of this system that has a frequency range from 0.02Hz to 146Hz. The frequency range of the velocity-based MEMS wider than the geophone that has a frequency range from 10Hz to 100Hz. According to these, the velocity-based MEMS system is better able to detect low-frequency vibration signals. The low-frequency vibration signals required for data in monitoring seismic activity. Therefore, the velocity-based MEMS system is suitable as the seismometer especially velocity-based seismometer.

ACKNOWLEDGMENT

The authors would like to thank to all members of Measurement Circuit and System Research Laboratory, Brawijaya University, and who has supported the implementation of this research.

REFERENCES

- [1] T. Deng, D. Chen, J. Wang, J. Chen, dan W. He, "A MEMS based electrochemical vibration sensor for seismic motion monitoring," *J. Microelectromechanical Syst.*, vol. 23, no. 1, hal. 92–99, 2014.
- [2] G. Li *et al.*, "A MEMS based seismic sensor using the electrochemical approach," *Procedia Eng.*, vol. 47, hal. 362–365, 2012.
- [3] G. Li, J. Wang, D. Chen, J. Chen, L. Chen, dan C. Xu, "An electrochemical, low-frequency seismic micro-sensor based on MEMS with a force-balanced feedback system," *Sensors (Switzerland)*, vol. 17, no. 9, 2017.
- [4] R. Brincker, B. Bolton, A. Brandt, B. Allé, dan D.-O. M, "Calibration and Processing of Geophone Signals for Structural Vibration Measurements," in *Experimental Mechanics*, 2010, hal. 1–5.
- [5] M. Hons, "Seismic sensing: Comparison of geophones and accelerometers using laboratory and field data," 2008.
- [6] M. S. Hons, R. R. Stewart, G. Hauer, D. C. Lawton, dan M. B. Bertram, "Accelerometer Versus Geophone Response - A Field Case History," 2008, no. June.
- [7] J. Lainé dan D. Mougnot, "A high-sensitivity MEMS-based accelerometer," no. November, 2014.
- [8] J. Laine dan D. Mougnot, "Benefits Of MEMS Based Seismic Accelerometers For Oil Exploration," in *Transducers & Eurosensors*, 2007, hal. 1473–1477.
- [9] T. Aizawa, T. Kimura, T. Matsuoka, T. Takeda, dan Y. Asano, "Application of MEMS accelerometer to geophysics," *Int. J. JCRM*, vol. 4, no. 2, hal. 33–36, 2008.
- [10] D. R. Santoso, S. Maryanto, dan A. Nadhir, "Application of Single MEMS-accelerometer to Measure 3-axis Vibrations and 2-axis Tilt-Angle Simultaneously," *TELKOMNIKA*, vol. 13, no. 2, hal. 442, 2015.
- [11] Texas Instruments, "LF444 Quad Low Power JFET Input Operational Amplifier LF444 Quad Low Power JFET Input Operational Amplifier," 1995. .
- [12] P. Tapashetti, A. Gupta, C. Mithlesh, dan A. S. Umesh, "Design and Simulation of Op Amp Integrator and Its Applications," no. 3, hal. 12–19, 2012.
- [13] R. Hossain, M. Ahmed, H. U. Zaman, dan M. A. Nazim, "A Comparative Study of Various Simulation Software for Design and Analysis of Operational Amplifier Based Integrator Circuits," hal. 278–282, 2017.